

Explosive information spreading in higher-order networks: Effect of social reinforcement

Yu Zhou(周宇), Yingpeng Liu(刘英鹏), Liang Yuan(袁亮), Youhao Zhuo(卓友濠), Kesheng Xu(徐克生), Jiao Wu(吴娇), and Muhua Zheng(郑木华)

Citation: Chin. Phys. B, 2025, 34 (**3**): 038704. DOI: 10.1088/1674-1056/adacc8
Journal homepage: http://cpb.iphy.ac.cn; http://iopscience.iop.org/cpb

What follows is a list of articles you may be interested in

Effects of individual heterogeneity on social contagions

Fu-Zhong Nian(年福忠) and Yu Yang(杨宇)
Chin. Phys. B, 2024, 33 (**5**): 058705. DOI: 10.1088/1674-1056/ad225e

Dynamical behaviors in discrete memristor-coupled small-world neuronal networks

Jieyu Lu(鲁婕妤), Xiaohua Xie(谢小华), Yaping Lu(卢亚平), Yalian Wu(吴亚联), Chunlai Li(李春来), and Minglin Ma(马铭磷)
Chin. Phys. B, 2024, 33 (**4**): 048701. DOI: 10.1088/1674-1056/ad1483

Studying the co-evolution of information diffusion, vaccination behavior and disease transmission in multilayer networks with local and global effects

Liang'an Huo(霍良安) and Bingjie Wu(武兵杰)
Chin. Phys. B, 2024, 33 (**3**): 038702. DOI: 10.1088/1674-1056/ad0114

Impact of individual behavior adoption heterogeneity on epidemic transmission in multiplex networks

Liang'an Huo(霍良安) and Yue Yu(于跃)
Chin. Phys. B, 2023, 32 (**10**): 108703. DOI: 10.1088/1674-1056/acea65

Modeling for heterogeneous multi-stage information propagation networks and maximizing information

Ren-Jie Mei(梅人杰), Li Ding(丁李), Xu-Ming An(安栩明), Ping Hu(胡萍)
Chin. Phys. B, 2019, 28 (**2**): 028701. DOI: 10.1088/1674-1056/28/2/028701

RAPID COMMUNICATION

Explosive information spreading in higher-order networks: Effect of social reinforcement

Yu Zhou(周宇)[1], Yingpeng Liu(刘英鹏)[1], Liang Yuan(袁亮)[1], Youhao Zhuo(卓友濠)[1], Kesheng Xu(徐克生)[1], Jiao Wu(吴娇)[2,†], and Muhua Zheng(郑木华)[1]

[1] *School of Physics and Electronic Engineering, Jiangsu University, Zhenjiang* 212013, *China*
[2] *School of Mathematical Sciences, Jiangsu University, Zhenjiang* 212013, *China*

(Received 17 December 2024; revised manuscript received 14 January 2025; accepted manuscript online 22 January 2025)

Information spreading has been investigated for many years, but the mechanism of why the information explosively catches on overnight is still under debate. This explosive spreading phenomenon was usually considered driven separately by social reinforcement or higher-order interactions. However, due to the limitations of empirical data and theoretical analysis, how the higher-order network structure affects the explosive information spreading under the role of social reinforcement has not been fully explored. In this work, we propose an information-spreading model by considering the social reinforcement in real and synthetic higher-order networks, describable as hypergraphs. Depending on the average group size (hyperedge cardinality) and node membership (hyperdegree), we observe two different spreading behaviors: (i) The spreading progress is not sensitive to social reinforcement, resulting in the information localized in a small part of nodes; (ii) a strong social reinforcement will promote the large-scale spread of information and induce an explosive transition. Moreover, a large average group size and membership would be beneficial to the appearance of the explosive transition. Further, we display that the heterogeneity of the node membership and group size distributions benefit the information spreading. Finally, we extend the group-based approximate master equations to verify the simulation results. Our findings may help us to comprehend the rapidly information-spreading phenomenon in modern society.

Keywords: explosive information spreading, social reinforcement, higher-order interactions, complex network

PACS: 87.23.Ge, 64.60.aq

DOI: 10.1088/1674-1056/adacc8 **CSTR:** 32038.14.CPB.adacc8

1. Introduction

The investigations of network propagation dynamics have attracted considerable attention and have made many outstanding progresses,[1–8] such as the discovery of a very small critical threshold,[9–11] diverse contagion patterns,[12,13] different propagation modes,[14,15] influence maximization[16,17] etc. However, the underlying mechanisms of why information, opinions, gossip, innovation, and products unexpectedly develop famous overnight have not been fully understood.[14] It is commonly accepted that explosive information spreading can properly explain this phenomenon, in which there is a discontinuous transition related to some pivotal characteristics, such as the threshold model,[18,19] synergistic and memory effects,[14,15,20] and so on.[21,22] The findings have greatly improved our knowledge of the explosive spreading mechanisms.

Research has shown one of the essential characteristics that contribute to the explosive spreading phenomenon, namely, social reinforcement — an individual needs to confirm the reliability of the information many times from neighbors before accepting it.[23–27] It has shown that the model considering social reinforcement can describe the online behavior-spreading experiments and the sudden events spreading patterns on Sina Weibo very well.[28,29] In addition, a strong social reinforcement will accelerate the spread and lead to a discontinuous transition in the phase diagram.

The majority of models usually focus on pairwise interactions between individuals, which are structurally represented by the network links. However, to the best of our knowledge, pairwise interactions are often insufficient to describe the information-spreading processes, such as adopting behaviors or novelties. Beyond typical pairwise interactions, the information can be spread via higher-order interactions (i.e., group interactions).[30–34] Recently, researchers found that there is an explosive spreading phenomenon in which the phase transition becomes discontinuous with the increasing strength of group interactions.[30–34] For example, Iacopini *et al.*[30] introduced a spreading model with group interactions and found a discontinuous transition as well as a hysteresis loop in the phase diagram. Guillaume *et al.*[35] demonstrated the influence of large groups and showed a continuous or discontinuous phase transition with a bistable region. Researchers in the complex network field have turned their attention to higher-order network models.[33–40] Now, an interesting question arises: Com-

†Corresponding author. E-mail: wujiao@ujs.edu.cn

© 2025 Chinese Physical Society and IOP Publishing Ltd. All rights, including for text and data mining, AI training, and similar technologies, are reserved.

bining the higher-order interactions with social reinforcement to the model, does the explosive transition certainly occur in the information-spreading process? In other words, how does the higher-order network structure affect the explosive information spreading under the roles of social reinforcement? We know little about the answer due to the limitations of empirical data and corresponding analytical approaches.

Inspired by the above question, we acquire some representative higher-order network data and propose a susceptible–infected–recovered (SIR) information-spreading model considering the social reinforcement on empirical and synthetic higher-order networks. We utilize the bipartite representation of hypergraphs to depict the higher-order interactions. In particular, we use a bipartite graph's two kinds of vertices to represent the sets of hypergraph nodes and groups.[33] Moreover, we develop group-based approximate master equations (AMEs)[35,41–46] for our model to understand the underlying mechanism. We observe two different spreading behaviors on real-world hypergraphs: (i) The spreading process is not sensitive to social reinforcement, resulting in the information localized in a small part of nodes; (ii) a strong social reinforcement will promote the large-scale spread of information and induce an explosive transition. Our results show that the network's average group size and membership are the major contributors to these two spreading behaviors. A sizeable average group size and membership would benefit the appearance of the explosive transition. Additionally, we display that the heterogeneity of membership and group size distributions are very helpful for spreading information under higher-order interactions.

We manage this paper as follows. Section 2 depicts the empirical higher-order network data. Section 3 proposes the SIR model with social reinforcement on the higher-order networks. We then develop the group-based approximate master equations for our model in Section 4. Section 5 presents our simulation and theoretical results. Finally, we give a conclusion in Section 6.

2. Data description

We obtain the empirical higher-order network data from Ref. [47]. Since the original hypergraphs include plenty of nodes and groups, which is too difficult and expensive to simulate the model, we use the same method in Ref. [35] to extract the sub-hypergraphs. In particular, we use the breadth-first search algorithm with a maximum distance of 2 to obtain the sub-hypergraphs. In this way, we obtain a connected sub-hypergraph from the original network. The description of the representative empirical higher-order networks is as follows.

Threads-ask-ubuntu (TAU) TAU is the user interaction dataset from the stack exchange websites.[33] Users post answers to questions, constructing a question-and-answer "thread". The nodes are users, and the group corresponds to the set of users asking a question or posting an answer on a single thread.

Threads-math-sx (TMS) TMS is a user interaction dataset from the stack exchange websites.[33] Nodes represent users, and groups correspond to the users asking a question or posting an answer on a single thread.

Coauth-MAG-geology (Geology) The geology dataset is derived from all papers classified under the "geology" field of study in the Microsoft Academic Graph (MAG).[48] In this dataset, the nodes correspond to the authors, and a group of size n represents n authors on a scientific publication.

Coauth-DBLP (DBLP) DBLP is an online bibliography that contains information about the publications and authors in influential computer science journals and proceedings.[35,47,49] In this network, each node represents an author, and a group of size n stands for the collaboration of n coauthors in the same publication.

Table 1 lists the main properties of each considered network.

Table 1. Overview of the considered higher-order networks. From left to right, each column represents the network name, number of nodes N, number of groups G, the exponent of the power-law membership distribution γ_m, average membership $\langle m\rangle$, maximum membership $m_{\max}$, average group size $\langle n\rangle$, and maximum group size $n_{\max}$.

Name	N	G	γ_m	$\langle m\rangle$	$m_{\max}$	$\langle n\rangle$	$n_{\max}$
TAU	77779	108927	2.0	3.26	2,247	2.32	14
TMS	152135	562447	1.8	9.54	12403	2.58	21
Geology	228384	200362	1.9	4.17	848	4.75	25
DBLP	57501	55204	2.3	3.75	903	3.90	25

3. The SIR model on higher-order networks

In our work, we take bipartite hypergraphs to describe the higher-order networks in which the bipartite graph's two kinds of vertices represent the sets of hypergraph nodes and groups, respectively. A hypergraph is a typical representation of the higher-order network. This enables the representation of more complex relationships and interactions, where a single hyperedge can capture multi-node connections that are often found in systems with higher-order interactions. As shown in Fig. 1(a), black circles indicate the groups, and white dots represent individuals or nodes. The group size n represents the number of nodes contained in a group, which is analogous to the hyperedge cardinality. The membership m indicates the number of groups a node belongs to. For example, in Fig. 1(a), we highlight a group with size $n = 6$ in orange and a node with membership $m = 2$ in blue. For simplicity, we denote the distributions of group size n and membership m with p_n and g_m, respectively.

To study the impact of higher-order networks on explosive information spreading, we introduce a SIR information spreading model with social reinforcement (see Fig. 1(b)). Every node in the network can stay in susceptible (S), infected

(I), or recovered (R) state (indicated by different colors in Fig. 1(b)). If a size n group has i infected nodes (with $i \leq n$), the infected probability $\beta(n,i)$ for each S state node in the group can take the following form as in the literature:[23,50]

$$\beta(n,i) = \begin{cases} 1-(1-\lambda)(1-b)^{i-1}, & \lambda \in (0,1], b \in [0,1], \\ 0, & \lambda = 0, i = 0, \end{cases} \quad (1)$$

where λ and b represent the primary spreading probability and social reinforcement, respectively. The primary spreading probability is also called information sensitivity, which reflects the level of sensitivity of a node receiving the information for the first time.[23,29] The individual is more susceptible to the information and prefers to believe it when λ is larger. In addition, there is no social reinforcement when $b = 0$, whereas the degree of social reinforcement becomes extremely strong at $b = 1$. In other words, the individual is more sensitive to the impact of neighbors in the same group and is more likely to become infected at a larger b. Note that by considering these two factors, the model is able to effectively replicate Centola's behavior spreading experiments,[28] where it was observed that, with stronger social reinforcement, information diffusion occurs more rapidly and extensively in regular networks compared to random networks.[23] Additionally, this model can accurately mirror the spreading patterns observed in six notable events on Sina Weibo.[29] In fact, more results may be obtained if we can consider another model by incorporating more factors to $\beta(n,i)$.[35] We here use the social reinforcement model to study the explosive information spreading on higher-order networks due to its excellent ability to reproduce the real spreading phenomena.

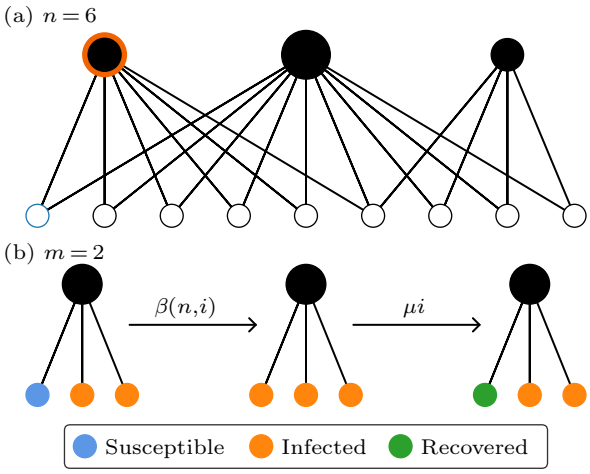


Fig. 1. The SIR model on the higher-order network. (a) We utilize a bipartite graph to represent the higher-order structure. White circles represent the nodes or individuals, and black ones indicate the groups to which the nodes belong. We highlight a group with size $n = 6$ in orange and a node with membership $m = 2$ in blue. (b) If a group with size n has i infected nodes (with $i \leq n$), each susceptible node in this group evolves to the infected state with probability $\beta(n,i)$ as Eq. (1). Each infected node independently turns to the recovered state with probability μ.

Notice that since nodes can belong to multiple groups, we calculate the total transition rate for the susceptible nodes by summing up the infection rates related to each group (i.e., the infection process is independent). All infected nodes independently turn to the recovered state with a fixed probability μ. Without loss of generality, we set $\mu = 1$ in this work.

We implement our SIR model on hypergraphs using the standard Gillespie algorithm for numerical simulation. We initially choose a ratio ρ_0 of nodes as seeds and set them as infected states. The remains are in the susceptible states. We can divide the processes into $j \in J$ events, where each event can be of two types: infection or recovery. If a group with size n has i infected nodes and r recovered nodes, we select this group for the infection event with rate $\omega_{\text{inf}} = (n-i-r)\beta(n,i)$. Once we select a group for the infection event, we then randomly choose one susceptible node with an equal probability from set $n-i-r$ and turn it to the infected state. Meanwhile, the rate in the recovery event for all infected nodes is $\omega_{\text{rec}} = 1$. Therefore, the happening probability of each event is $P(j) = \frac{\omega_j}{\sum_{j\in J}\omega_j}$. The time step between two events Δt takes from an exponential distribution with average $\langle \Delta t \rangle = \frac{1}{\sum_{j\in J}\omega_j}$. After each event occurs, the rate ω_{inf} should be updated accordingly.

4. A theoretical analysis based on group-based AMEs

To better understand the effects of higher-order interactions on information spreading, we develop group-based AMEs[41–46] to examine the numerical simulations. The group-based AMEs were first developed to analyze the susceptible–infected–susceptible epidemic spreading model.[41–46] Now, we extend this theory to our SIR model as the current concern.[51] To track the information-spreading process, we define $I_m(t)$ ($S_m(t)$) as the infected (susceptible) nodes' densities with membership m at time t. Meanwhile, we utilize $F_{n,i}(t)$ to represent the fraction of groups with effective size n containing i infected nodes at time t. Notice that the effective size n is not fixed anymore and is characterized as the sum of susceptible and infected nodes in a group. Therefore, the effective size n will decrease by $n \mapsto n-1$ if an infected node recovers.

Next, we can calculate the following two critical rates. First, for a susceptible node, the average infection rate caused by a randomly chosen group to which this node belongs is

$$r(t) = \frac{\sum_{n,i}\beta(n,i)(n-i)F_{n,i}(t)}{\sum_{n,i}(n-i)F_{n,i}(t)}. \quad (2)$$

Herein, the sums over m or n cover each value as long as $g_m > 0$ or $p_n > 0$, and the sum over i is calculated from 0 to n.

Second, we randomly select a node in a susceptible state within a group. Besides the group from which we chose the node, we can obtain the average infection rate donated from

all the outer groups with

$$\rho(t) = r(t)\frac{\sum_m m(m-1)S_m(t)}{\sum_m mS_m(t)}. \tag{3}$$

Based on Eqs. (2) and (3), we can get the system's AMEs:

$$\frac{\mathrm{d}I_m}{\mathrm{d}t} = -\mu I_m + mrS_m, \tag{4}$$

$$\frac{\mathrm{d}S_m}{\mathrm{d}t} = -mrS_m, \tag{5}$$

$$\begin{aligned}\frac{F_{n,i}}{\mathrm{d}t} &= \mu(i+1)F_{n+1,i+1} - \mu i F_{n,i} - (n-i)\left[\beta(n,i)+\rho\right]F_{n,i} \\ &\quad +(n-i+1)\left[\beta(n,i-1)+\rho\right]F_{n,i-1}.\end{aligned} \tag{6}$$

From Eqs. (4)–(6), we can calculate the global fractions of susceptible, infected, and recovered nodes as

$$S(t) = \sum_m S_m(t), \tag{7}$$

$$I(t) = \sum_m I_m(t), \tag{8}$$

$$R(t) = 1 - I(t) - S(t) = 1 - \sum_m \left[I_m(t) + S_m(t)\right]. \tag{9}$$

Our theoretical results mainly come from Eqs. (7)–(9), which are solved by numerical integration with initial conditions $I_m(0) = g_m\rho_0$, $S_m(0) = g_m(1-\rho_0)$, $F_{n,i}(0) = \binom{n}{i}\rho_0^i(1-\rho_0)^{n-i}p_n$, where ρ_0 is the initial infection ratio of nodes. We examine the effects of higher-order network structure on the explosive information spreading under social reinforcement and show the related theoretical curves in the figures.

5. Results

5.1. Information spreading on real-world hypergraphs

We perform our SIR model on real-world hypergraphs to examine the influence of higher-order interactions. In order to better track the evolution process, we denote $\rho_S(t)$ ($\rho_I(t)$ and $\rho_R(t)$) as the fraction of nodes with S (I and R) states at time t. When the contagion ends, we use $\rho_R(\infty)$ to define the final fraction of recovered nodes. In fact, $\rho_R(\infty)$ also reflects the final spreading range, and an enormous value means a broader information scope.

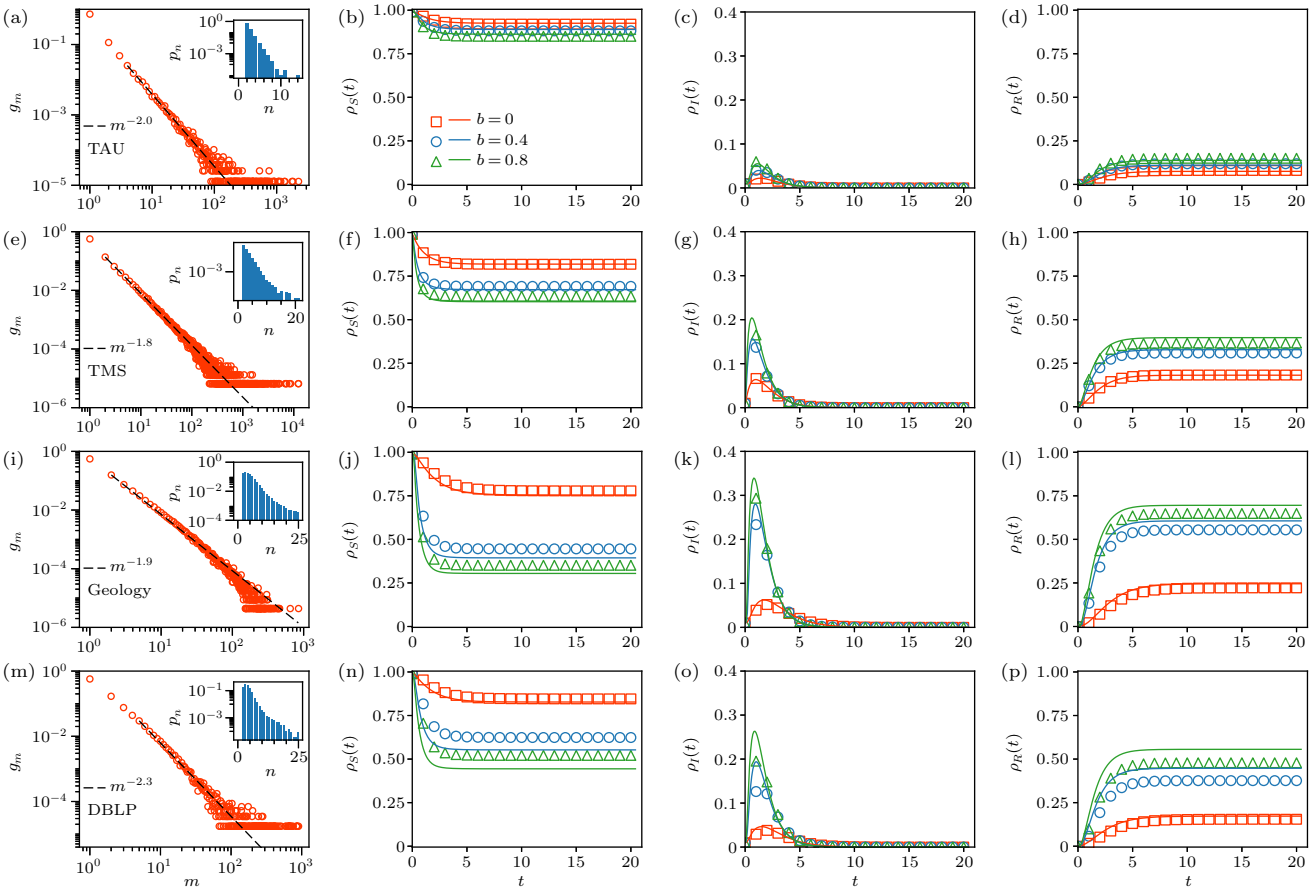


Fig. 2. Information spreading on real-world hypergraphs. Each row in the figure represents the results of one real-world hypergraph. The first column shows the membership distribution g_m and the group size distribution p_n (inset). The dashed line indicates the power law fitting with $g_m \sim m^{-\gamma_m}$. The second to fourth columns display the time evolution of the fraction of susceptible, infected, and recovered nodes, respectively. The symbols show the simulation results and the solid curves stand for the theoretical solutions from Eqs. (7)–(9). Red, blue, and green on the symbols and lines indicate the levels of social reinforcement $b = 0.0$, $b = 0.4$, and $b = 0.8$. We obtain each numerical simulation result by average 100 independent realizations and set other parameters as $\rho_0 = 0.01$ and $\lambda = 0.05$.

As shown in Fig. 2, the membership distribution g_m in all real-world networks is heterogeneous, which approximately follows a power-law form $g_m \sim m^{-\gamma_m}$ (see the power law fitting in the dashed line). The distribution of group size n is more homogeneous than the membership m. Table 1 summarizes the exponent of the power-law membership distribution γ_m, the average membership $\langle m \rangle$, maximum membership $m_{\max}$, average group size $\langle n \rangle$, and maximum group size $n_{\max}$ for each network.

The time evolutions of the susceptible, infected, and recovered nodes' fractions differ due to the structure difference in real-world hypergraphs (see the second to fourth columns of Fig. 2). We find a curious phenomenon in network TAU — even though we have increased the social reinforcement to $b = 0.8$, as shown in Figs. 2(b)–2(d), the information is still localized in a small part of nodes. In the end, $\rho_R(t)$ eventually stabilizes at a very low value (i.e., only 13.8% nodes accept the information). However, we observe a different spreading behavior in network TMS, Geology and DBLP. As shown in Fig. 2, when the social reinforcement is very strong, the $\rho_S(t)$ decreases faster, the peak of $\rho_I(t)$ is higher, and $\rho_R(t)$ increases rapidly. The spreading behavior is very sensitive to social reinforcement in these networks, which implies that a strong social reinforcement will result in the large-scale spread of information. The theoretical results from Eqs. (7)–(9) conform with the simulations very well. This phenomenon implies that some network structure characteristics influence the information spreading under social reinforcement.

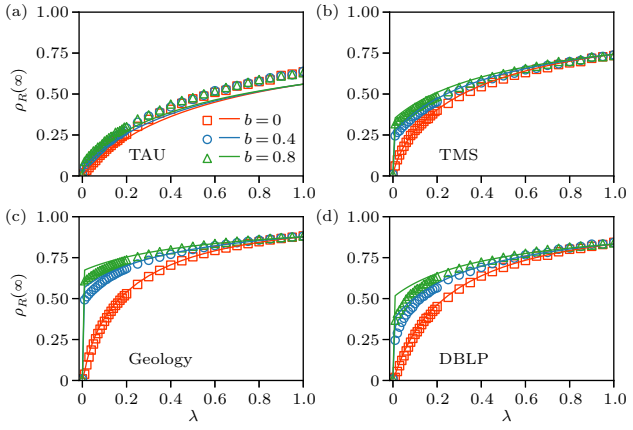


Fig. 3. Two different spreading transitions with a large social reinforcement. $\rho_R(\infty)$ versus λ in different real networks. The symbols show the simulation results and the solid curves stand for the theoretical solutions from Eqs. (7)–(9). We obtain each numerical simulation result by average 100 independent realizations and set $\rho_0 = 0.01$.

Besides the time evolution processes, we also investigate the association between the final spreading range $\rho_R(\infty)$ and the primary spreading rate λ with different social reinforcement in real networks. From Fig. 3(a), we can see that the final spreading range is not sensitive to social reinforcement in network TAU. No matter how strong the social reinforcement is, the final spreading range versus the primary spreading rate shows a continuous transition. However, in Figs. 3(b)–3(d), the explosive transition emerges with a large social reinforcement, where there exists an abrupt transition. Our theoretical results from Eqs. (7)–(9) conform with the numerical simulations very well.

The above findings have greatly piqued our interest and motivated us to examine which key factors contribute to the explosive spreading behaviors in the higher-order networks. Table 1 shows that the average group size $\langle n \rangle$ and membership $\langle m \rangle$ are the smallest in network TAU. Intuitively, the average group size and membership strongly influence the spreading of information. Next, we will examine the impact of the average group size $\langle n \rangle$ and membership $\langle m \rangle$ on the spreading behaviors in detail.

5.2. The impact of the average group size $\langle n \rangle$ and average membership $\langle m \rangle$

To better understand how the two different spreading transitions show up, we perform our model in a large number of synthetic higher-order networks with varying average group sizes and memberships. As the distribution of membership g_m and group size p_n can be homogeneous or heterogeneous, we consider the homogeneous case of $g_m = \delta_{m,\langle m \rangle}$ and $p_n = \delta_{n,\langle n \rangle}$, and the heterogeneous case as $g_m \sim m^{-\gamma_m}$ and $p_n \sim n^{-\gamma_n}$. We use the configuration model on hypergraph with bipartite structure to generate the synthetic networks. In particular, we first create a group sequence from the distribution p_n and a membership sequence from g_m. Note that the sum of the group sequence must be equal to the sum of the membership sequence (i.e., $\sum_n nGp_n = \sum_m mNg_m$). Then, we randomly shuffle both sequences and pair them to form the edge list, i.e., node and group associations. In addition, we adopt edge swaps to destroy multi-edges.[52] Finally, we obtain a synthetic hypergraph with the desired properties.

In Fig. 4, we explore the association between the final spreading coverage $\rho_R(\infty)$ and the primary spreading rate λ with different average group size $\langle n \rangle$ and average membership $\langle m \rangle$. Considering the group size distribution $p_n = \delta_{n,\langle n \rangle}$, we examine the effect of average group size $\langle n \rangle$ on explosive transition by fixing $g_m = \delta_{m,3}$ in Fig. 4(a) and $g_m \sim m^{-2.1}$, $\langle m \rangle = 3$ in Fig. 4(b). We can see that no matter whether the distribution g_m is homogeneous or heterogeneous, a sizeable average group size $\langle n \rangle$ will induce the emergence of the explosive transition, characterized by an abrupt transition. Interestingly, the information spreading shows a continuous transition on the network with a small group size $\langle n \rangle$, which is similar to the observation on network TAU in Fig. 3(a). As a susceptible node knows the whole group nodes' states, a large group size will make the effect of group interactions more evident, which can be interpreted as compensation for social reinforcement. This result implies that the average group size $\langle n \rangle$ is a key factor for the explosive transition in information spreading.

Besides the group size, we also examine the effect of average membership $\langle m \rangle$ on explosive transition in Figs. 4(c)

and 4(d). We fix $p_n = \delta_{n,4}$ and show our results of homogeneous distribution $g_m = \delta_{m,\langle m\rangle}$ in Fig. 4(c) and heterogeneous $g_m \sim m^{-2.1}$ in Fig. 4(d). We find that a large average membership $\langle m\rangle$ will promote explosive transition in the information spreading process. As the nodes with a large membership have more chance to receive the information, a large average membership $\langle m\rangle$ will make the information spread to an extensive scale. Thus, the average membership $\langle m\rangle$ is another critical factor affecting the range of information spreading.

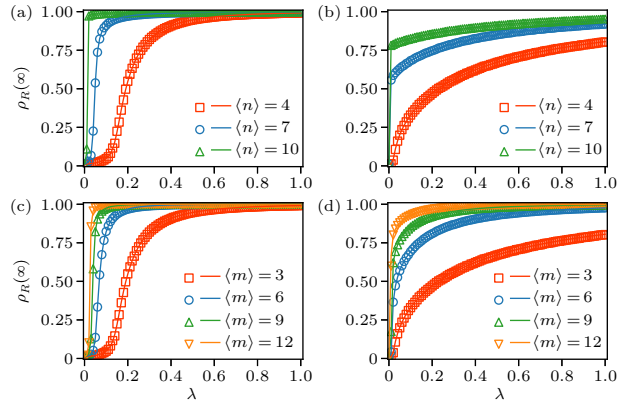


Fig. 4. Explosive transition induced by a large average group size and membership. (a) $\rho_R(\infty)$ vs. λ for different average group sizes $\langle n\rangle$. The membership distribution of the networks is fixed as $g_m = \delta_{m,3}$ and the distribution of group size is $p_n = \delta_{n,4}$, $\delta_{n,7}$ and $\delta_{n,10}$, respectively. (b) same as (a) but given $g_m \sim m^{-2.1}$ and $\langle m\rangle = 3$; (c) $\rho_R(\infty)$ vs. λ for different average group sizes $\langle m\rangle$. We fix $p_n = \delta_{n,4}$ and set $g_m = \delta_{m,3}$, $\delta_{m,6}$, $\delta_{m,9}$ and $\delta_{m,12}$, respectively. (d) same as (c) but $g_m \sim m^{-2.1}$. The symbols show the simulation results and the solid curves stand the theoretical solutions from Eqs. (7)–(9). We obtain each numerical simulation result by average 100 independent realizations and set $\rho_0 = 0.01$ and $b = 0.4$.

5.3. The impact of the distributions of the membership and group size

After thorough comparison and analysis in Fig. 4, we discover that the network with heterogeneous membership distribution will accelerate the information propagation under a small λ. To clarify, figure 5 shows the time evolution $\rho_R(t)$ on the synthetic networks with different membership distributions g_m. Comparing with Figs. 5(a) and 5(b), we can see that the information can not spread out in homogeneous g_m for different b. However, the spreading range gradually expands as b increases in the heterogeneous case. For $\langle m\rangle = 6$, we observe a similar phenomenon of the heterogeneous membership distribution promoting the spreading in Figs. 5(c) and 5(d). These results indicate that the heterogeneity of membership distribution benefits the information propagation.

The above observation raises another question: Does the group size distribution p_n influence information propagation? In Figs. 6(a) and 6(b), we show the time evolution $\rho_R(t)$ on the networks with homogeneous $p_n = \delta_{n,4}$ and heterogeneous $p_n \sim n^{-2.5}$, $\langle n\rangle = 4$, respectively. Comparing with Figs. 6(a) and 6(b), we find that even though the social reinforcement $b = 1$, the information can not be spread out on the network with homogeneous group size distribution at a small λ. However, in the heterogeneous case, the information can be contagious to a certain percentage of individuals with the same λ, and a large social reinforcement will facilitate the spreading of information. Besides the time evolution, in Figs. 6(c) and 6(d), we also study the final fraction of recovered nodes in parameter space (λ, b) with the same networks in Figs. 6(a) and 6(b), respectively. We show that with small λ and b, the information will spread globally in the network with a heterogeneous group size distribution. The results imply that the information is maintained in large groups. In fact, our results are consistent with the previous findings — heterogeneous group sizes promote a mesoscopic localization regime where the large groups sustain contagion.[35,45,46]

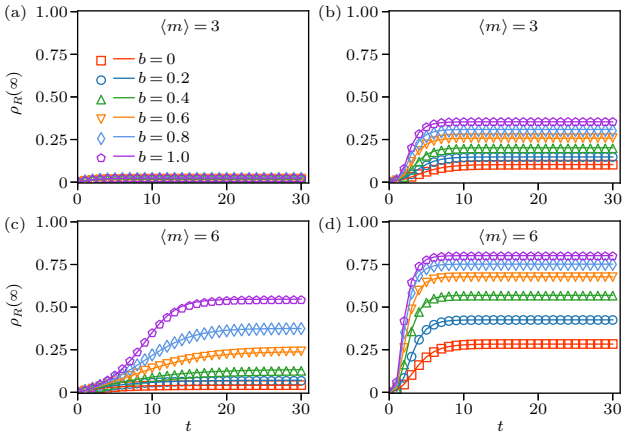


Fig. 5. The effect of the distribution of the membership on information spreading. Time evolution of $\rho_R(t)$ on the synthetic networks with different membership distributions g_m. Left and right columns show the network with homogeneous $g_m = \delta_{m,\langle m\rangle}$ and heterogeneous $g_m \sim m^{-2.1}$, respectively. The average membership $\langle m\rangle = 3$ in panels (a), (b) and $\langle m\rangle = 6$ in panels (c), (d). The symbols show the simulation results and the solid curves stand for the theoretical solutions from Eqs. (7)–(9). Other parameters are set as $p_n = \delta_{n,4}$, $\lambda = 0.05$, and $\rho_0 = 0.01$.

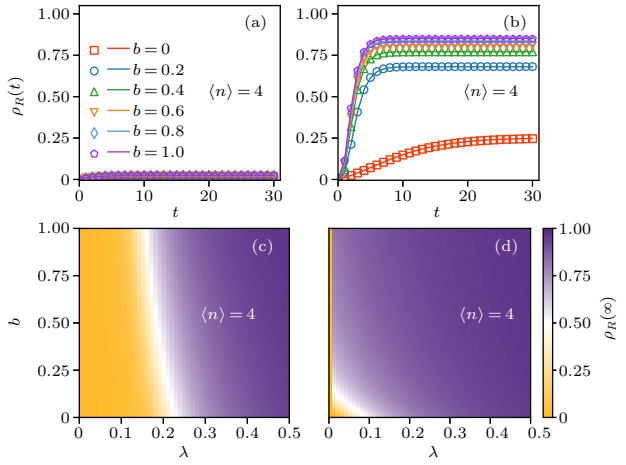


Fig. 6. Impact of group size distribution on information spreading. (a) and (b) The time evolution of $\rho_R(t)$ in the networks with homogeneous $p_n = \delta_{n,4}$ and heterogeneous $p_n \sim n^{-2.5}$, respectively. Here, $\lambda = 0.05$ is fixed. The symbols show the simulation results and the solid curves stand for the theoretical solutions from Eqs. (7)–(9). (c) and (d) The final spreading range from numerical simulations in parameter space (λ, b) with the corresponding networks in panels (a) and (b), respectively. We do not show the theoretical results here, as they agree with simulations very well. Other parameters are set as $g_m = \delta_{m,3}$ and $\rho_0 = 0.01$.

6. Conclusion

In the study of information spreading, researchers have found that social reinforcement is an essential characteristic driving the explosive spreading phenomenon.[23] In recent years, researchers discovered that the explosive spreading phenomenon was caused by higher-order interactions.[30–34] However, due to the limitations of empirical data and theoretical analysis, the influences of higher-order network structure on the explosive information spreading under the roles of social reinforcement are not thoroughly studied.

In this work, taking into account the social reinforcement in the information-spreading model, we discovered two distinct spreading behaviors on real-world hypergraphs: (i) The spreading process is not sensitive to social reinforcement, resulting in the information localized in a small part of nodes; (ii) a strong social reinforcement will promote the large-scale spread of information and cause an explosive transition. Our results showed that the average group size and average membership in the network are the major causes of these two spreading behaviors. A large average group size and average membership will promote the appearance of the explosive transition. Additionally, increasing the heterogeneity of membership and group size distributions will accelerate information spreading under higher-order interactions. Ultimately, we used group-based approximate master equations to demonstrate our numerical results. These discoveries may illustrate the rapid spread mechanisms of stylish fashion in the real world, such as news, opinion, gossip, innovation, etc.

Acknowledgments

Project supported by the National Natural Science Foundation of China (Grant Nos. 12305043 and 12165016), the Natural Science Foundation of Jiangsu Province (Grant No. BK20220511), and the Project of Undergraduate Scientific Research (Grant No. 22A684). M. Z. appreciates the support from the Jiangsu Specially-Appointed Professor Program.

References

[1] Pastor-Satorras R, Castellano C, Van Mieghem P and Vespignani A 2015 *Rev. Mod. Phys.* **87** 925
[2] Barrat A, Barthelemy M and Vespignani A 2008 *Dynamical processes on complex networks* (Cambridge university press)
[3] Wang W, Tang M, Stanley H E and Braunstein L A 2017 *Reports on Progress in Physics* **80** 036603
[4] Liu C, Zhan X X, Zhang Z K, Sun G Q and Hui P M 2015 *New J. Phys.* **17** 113045
[5] Zhang Z K, Liu C, Zhan X X, Lu X, Zhang C X and Zhang Y C 2016 *Physics Reports* **651** 1
[6] Zhu X, Ma J, Su X, Tian H, Wang W and Cai S 2019 *Complexity* **2019** 5920187
[7] Feng M, Cai S M, Tang M and Lai Y C 2019 *Nat. Commun.* **10** 3748
[8] Yang Z, Wu J, He J, Xu K and Zheng M 2023 *Chaos, Solitons & Fractals* **171** 113487
[9] Pastor-Satorras R and Vespignani A 2001 *Phys. Rev. E* **63** 066117
[10] Boguná M and Pastor-Satorras R 2002 *Phys. Rev. E* **66** 047104
[11] Wang W, Tang M, Zhang H F and Lai Y C 2015 *Phys. Rev. E* **92** 012820
[12] Nematzadeh A, Ferrara E, Flammini A and Ahn Y Y 2014 *Phys. Rev. Lett.* **113** 088701
[13] Wu J, Xu K, Zhang X and Zheng M 2022 *Chaos* **32** 083134
[14] Gómez-Gardeñes J, Lotero L, Taraskin S and Pérez-Reche F 2016 *Scientific Reports* **6** 19767
[15] Liu Q H, Wang W, Tang M, Zhou T and Lai Y C 2017 *Phys. Rev. E* **95** 042320
[16] Xie M, Zhan X X, Liu C and Zhang Z K 2023 *Information Processing & Management* **60** 103161
[17] Lü L, Chen D, Ren X L, Zhang Q M, Zhang Y C and Zhou T 2016 *Physics Reports* **650** 1
[18] Watts D J 2002 *Proc. Natl. Acad. Sci. USA* **99** 5766
[19] Centola D, Eguíluz V M and Macy M W 2007 *Physica A* **374** 449
[20] Dodds P S and Watts D J 2004 *Phys. Rev. Lett.* **92** 218701
[21] Assis V R and Copelli M 2009 *PPhys. Rev. E* **80** 061105
[22] Gross T, D'Lima C and Blasius B 2006 *Phys. Rev. Lett.* **96** 208701
[23] Zheng M, Lü L and Zhao M 2013 *Phys. Rev. E* **88** 012818
[24] Majumdar S N and Krapivsky P 2001 *Phys. Rev. E* **63** 045101
[25] de Kerchove C, Krings G, Lambiotte R, Van Dooren P and Blondel V 2009 *Phys. Rev. E* **79** 016114
[26] Onnela J P and Reed-Tsochas F 2010 *Proc. Natl. Acad. Sci. USA* **107** 18375
[27] Lü L, Chen D B and Zhou T 2011 *New J. Phys.* **13** 123005
[28] Centola D 2010 *Science* **329** 1194
[29] Wu J, Zheng M, Zhang Z K, Wang W, Gu C and Liu Z 2018 *Chaos* **28** 033113
[30] Iacopini I, Petri G, Barrat A and Latora V 2019 *Nat. Commun.* **10** 2485
[31] Matamalas J T, Gómez S and Arenas A 2020 *Phys. Rev. Research* **2** 012049
[32] Battiston F, Amico E, Barrat A, Bianconi G, Ferraz de Arruda G, Franceschiello B, Iacopini I, Kéfi S, Latora V, Moreno Y, *et al.* 2021 *Nat. Phys.* **17** 1093
[33] Battiston F, Cencetti G, Iacopini I, Latora V, Lucas M, Patania A, Young J G and Petri G 2020 *Physics Reports* **874** 1
[34] Boccaletti S, De Lellis P, del Genio C, Alfaro-Bittner K, Criado R, Jalan S and Romance M 2023 *Physics Reports* **1018** 1
[35] St-Onge G, Iacopini I, Latora V, Barrat A, Petri G, Allard A and Hébert-Dufresne L 2022 *Commun. Phys.* **5** 25
[36] Wang W, Nie Y, Li W, Lin T, Shang M S, Su S, Tang Y, Zhang Y C and Sun G Q 2024 *Physics Reports* **1056** 1
[37] Kim J H and Goh K I 2024 *Phys. Rev. Lett.* **132** 087401
[38] Landry N W, Thompson W, Hébert-Dufresne L and Young J G 2024 *Phys. Rev. E* **110** L042301
[39] Wang X, Wu J, Yang Z, Xu K, Wang Z and Zheng M 2024 *Physica A* **640** 129702
[40] Fang F, Ma J, Ma Y J and Boccaletti S 2024 *Chaos, Solitons & Fractals* **186** 115149
[41] Hébert-Dufresne L, Noël P A, Marceau V, Allard A and Dubé L J 2010 *Phys. Rev. E* **82** 036115
[42] O'Sullivan D J, O'Keeffe G J, Fennell P G and Gleeson J P 2015 *Frontiers in Physics* **3** 71
[43] Marceau V, Noël P A, Hébert-Dufresne L, Allard A and Dubé L J 2010 *Phys. Rev. E* **82** 036116
[44] Gleeson J P 2011 *Phys. Rev. Lett.* **107** 068701
[45] St-Onge G, Thibeault V, Allard A, Dubé L J and Hébert-Dufresne L 2021 *Phys. Rev. Lett.* **126** 098301
[46] St-Onge G, Thibeault V, Allard A, Dubé L J and Hébert-Dufresne L 2021 *Phys. Rev. E* **103** 032301
[47] Benson A R, Abebe R, Schaub M T, Jadbabaie A and Kleinberg J 2018 *Proc. Natl. Acad. Sci. USA* **115** E11221
[48] Sinha A, Shen Z, Song Y, Ma H, Eide D, Hsu B J and Wang K 2015 *Proceedings of the 24th International Conference on World Wide Web* pp. 243–246
[49] Patania A, Petri G and Vaccarino F 2017 *EPJ Data Science* **6** 18
[50] Wu J, Zheng M, Xu K and Gu C 2020 *Nonlinear Dyn.* **99** 2387
[51] St-Onge G, Hébert-Dufresne L and Allard A 2024 *Proc. Natl. Acad. Sci. USA* **121** e2312202121
[52] Fosdick B K, Larremore D B, Nishimura J and Ugander J 2018 *SIAM Review* **60** 315